

Research Article

Squaraine Planar-Heterojunction Solar Cells

Bin Fan, Ylenia Maniglio, Marina Simeunovic, Simon Kuster, Thomas Geiger, Roland Hany, and Frank Nüesch

Swiss Federal Laboratories for Materials Testing and Research, EMPA, Ueberlandstrasse 129, 8600 Dübendorf, Switzerland

Correspondence should be addressed to Bin Fan, bin.fan@empa.ch

Received 10 April 2009; Accepted 2 June 2009

Recommended by Mohamed Sabry Abdel-Mottaleb

The photovoltaic performance of squaraine-based organic solar cells is investigated. Two squaraine derivatives with extraordinarily high extinction coefficients are used as electron donors in bilayer heterojunctions with fullerene C₆₀ as electron acceptor. Due to the very strong squaraine absorption band in the red spectral domain, antibatic behavior due to light filtering is observed in the photocurrent spectrum for film thicknesses of 35 nm to 40 nm. At reduced film thicknesses of 20 nm, this filtering effect at maximum absorption can be alleviated and power conversion efficiencies under simulated AM 1.5 full sun irradiation of 0.59% and 1.01% are obtained for the two squaraine derivatives, respectively. The photovoltaic properties of these cells are investigated with respect to electrode materials and chemical doping.

Copyright © 2009 Bin Fan et al. This is an open access article distributed under the Creative Commons Attribution License, which permits unrestricted use, distribution, and reproduction in any medium, provided the original work is properly cited.

1. Introduction

The developments in organic semiconductors provide efficient and inexpensive solutions for solar energy conversion. Continuous optimization of organic solar cells has resulted in power conversion efficiencies (PCEs) from 4% to 5% for single junction cells based on spin-coated polymers [1] and thermally evaporated small molecules [2]. Compared to polymeric materials, small molecular semiconductors benefit from well-controlled synthesis and characterization along with easier purification [3–5]. Soluble small molecules are even more advantageous due to their low cost processability [6]. Several works have now demonstrated efficiencies above 1% in planar heterojunction cells [7], bulk-heterojunction cells, [8] and Schottky-type cells [9].

Among these soluble small molecular semiconductors, squaraine dyes are attracting a lot of attention due to their unique photophysical and photochemical properties. They are characterized by an aromatic four-membered ring system derived from squaric acid [10]. Their extinction coefficients are extraordinarily high and absorption in the far red and infrared domain has been demonstrated. Squaraine dyes that are solution-processible have already been applied in laser printers, photocopier, and optical disks as photoconductive materials [11, 12]. Their application in nonlinear optical

devices has also been investigated [13]. The exceptional optical properties of squaraines are of particular interest to solar cells. First of all, strong absorption coefficients open the possibility to use thinner active films, which may facilitate charge transport in the devices. Furthermore, there are only few organic materials absorbing so strongly in the far red and near infrared domain. Indeed, squaraines have already been employed quite early in organic Schottky-type solar cells, though with rather poor efficiency [14]. In recent years, squaraines have been extensively investigated in dye-sensitized solar cells (DSSCs) [15–20]. The best power conversion efficiency so far has reached 4.5% [21]. There are only few works that report on solid organic solar cells based on squaraines. Recently, a power conversion efficiency of 1.2% has been obtained in bulk-heterojunction solar cells using a blend of a squaraine derivative and (6,6)-phenyl C₆₁ butyric acid methylester (PCBM) [22].

To our best knowledge, bilayer heterojunction photovoltaic devices based on squaraines have not been reported so far. In this work, we report on planar-heterojunction solar cells based on two soluble squaraine derivatives, respectively, that we use as electron donors in combination with vacuum-deposited electron acceptor C₆₀. In particular, we investigate the influence of squaraine film thickness on the photovoltaic performance. We further improve device performance by

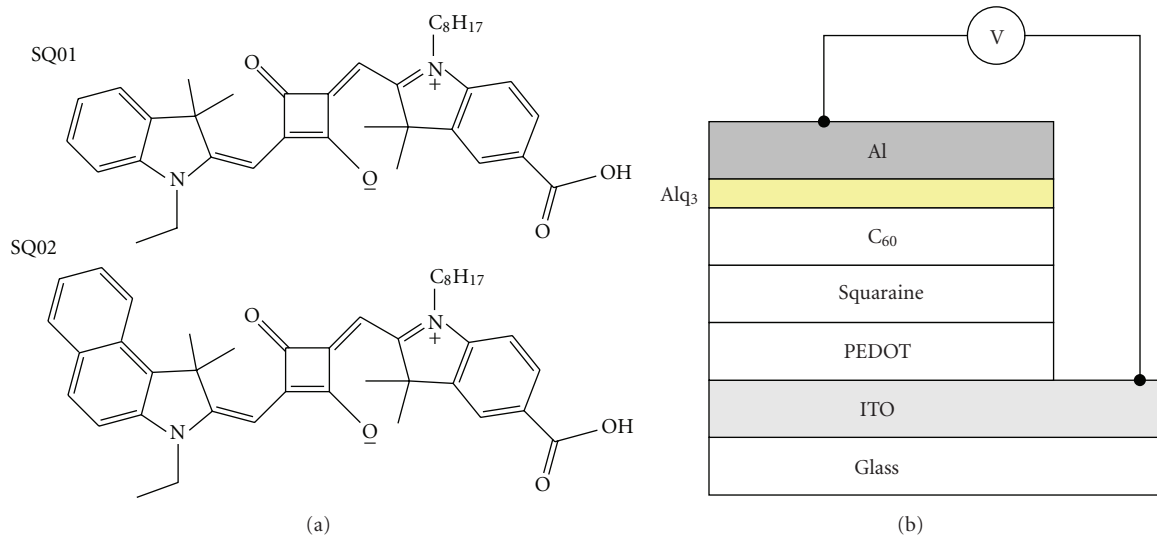


FIGURE 1: (a) Molecular structure of SQ01 and SQ02. (b) Solar cell architecture.

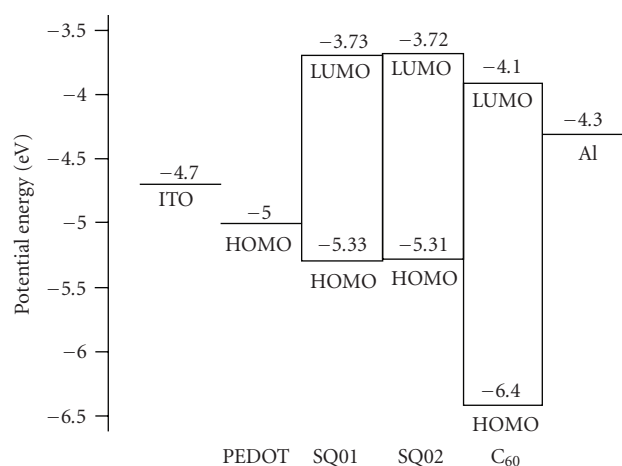


FIGURE 2: Energy level diagram of the organic materials and electrodes. The work function of Ca of -2.9 eV is not shown in this diagram.

choosing an appropriate cathode material. The effect of chemical doping of the squaraine layer is also investigated.

2. Experimental

The molecular structures of squaraine dyes SQ01 and SQ02 used in this work are shown in Figure 1(a). Both dyes were synthesized in our laboratory according to a previously published procedure [21] and exhibit extinction coefficients of approximately $300\,000\text{ L mol}^{-1}\text{ cm}^{-1}$ [23]. The architecture of our organic solar cells is shown in Figure 1(b). The indium tin oxide glass substrate (ITO, from AFC) was first cleaned in ozone plasma, then placed subsequently in acetone, ethanol, and soap ultrasonic baths, and finally dried in a nitrogen flow. A 50 nm thick layer of hole-transporting poly(styrene sulfonate) doped

poly (3,4-ethylenedioxythiophene) (PEDOT:PSS) (Sigma-Aldrich) was spin-coated on top of the ITO substrate from a water solution, then heated to 120°C for 15 minutes in order to remove residual water. The coated substrates were transferred into an N_2 glovebox to avoid exposure to oxygen and humidity. The squaraine dyes were spin-coated on top of the PEDOT:PSS layer from 5 mg/mL solutions in chloroform, resulting in layer thickness of 40 nm and 35 nm for SQ01 and SQ02, respectively. Thinner films of 20 nm were achieved by diluting the chloroform solutions accordingly. The C_{60} layer (40 nm) was vapor-deposited on top of the squaraine layer. Aluminum or calcium (60 nm) were used as top cathode to define an active device area of 7.1 mm^2 . Note that when applying aluminum as the cathode, an ultra-thin layer (2.5 nm) of tris(8-hydroxyquinoline)aluminum (Alq_3) was always inserted between Al and C_{60} as to protect the organic layers during aluminum deposition [24]. Alq_3 was not applied when calcium was used as cathode. To increase the conductivity of one of the squaraine films, SQ02 was doped with nitrosonium tetrafluoroborate (NO^+BF_4^-). Doping was first achieved in solution before coating the SQ02 solution to form a film. For that purpose, precise amounts of NO^+BF_4^- from a 0.01 mol/L NO^+BF_4^- master solution in CH_3CN were added to the SQ02 solutions in chloroform.

The energy level diagram of the organic materials and electrodes applied is shown in Figure 2. The levels of the highest occupied molecular orbitals (HOMOs) and lowest unoccupied molecular orbitals (LUMOs) of the squaraine dyes were determined by cyclic-voltammetry in dilute N,N-dimethylformamide (DMF) solutions using Fc/Fc^+ as an internal reference. The vacuum-referenced energy values were determined by adopting the potential of $+0.72\text{ V}$ versus NHE for Fc/Fc^+ in DMF and setting NHE at 4.5 eV below the zero vacuum energy level. The energy levels of the other materials are taken from our previous work [25].

The photovoltaic performances of the solar cells were measured under simulated AM 1.5 solar irradiation, with an

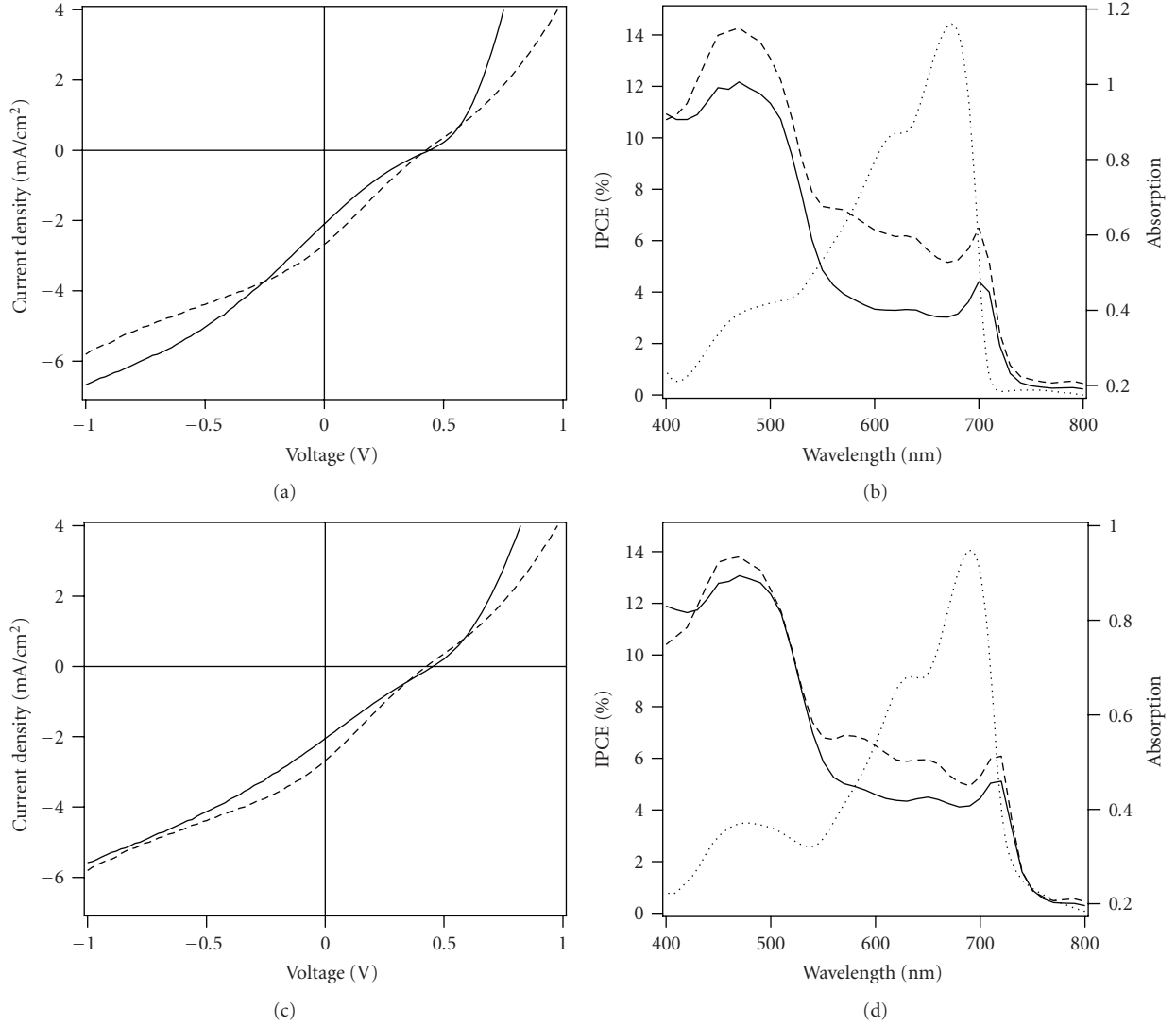


FIGURE 3: Current-voltage characteristics and IPCE curves of solar cells based on SQ01 ((a) and (b)) and SQ02 ((c) and (d)). The solid curves represent the cells using an Al/Alq₃ cathode, the dashed curves represent the cells using a Ca cathode. The dotted line in (b) and (d) represents the cell absorption. The thickness for SQ01 and SQ02 is 40 nm and 35 nm, respectively.

incident light intensity of $P_{in} = 100 \text{ mW/cm}^2$. The open-circuit voltage (V_{OC}) and short-circuit current (J_{SC}) were obtained directly from the current density-voltage (J - V) characteristics of the solar cells. The PCE is calculated as

$$\text{PCE}(\%) = \frac{\text{FF} \cdot V_{OC} \cdot J_{SC}}{P_{in}} \times 100\%, \quad (1)$$

with fill factor

$$\text{FF} = \frac{(J \cdot V)_{\max}}{V_{OC} \cdot J_{SC}}. \quad (2)$$

However, $(J \cdot V)_{\max}$ is the maximum power point and FF is the fill factor. The incident photon-to-current conversion efficiency (IPCE) is defined as the number of electrons

collected in the external circuit divided by the number of incident photons per second and is calculated according to

$$\text{IPCE}(\%) = \frac{hcJ_{SC}}{e\lambda P_{in}}, \quad (3)$$

where h is Planck's constant, c is the speed of light, e is the elementary charge, and λ is the monochromatic irradiation wavelength.

3. Results and Discussion

The J - V characteristics of solar cells using 40 nm thick SQ01 film or a 35 nm thick SQ02 film under AM 1.5 white light irradiation are shown in Figures 3(a) and 3(c), respectively. The photovoltaic parameters of these cells are summarized in Table 1. Comparing the photovoltaic performance of the two squaraines, we see that despite the structural difference

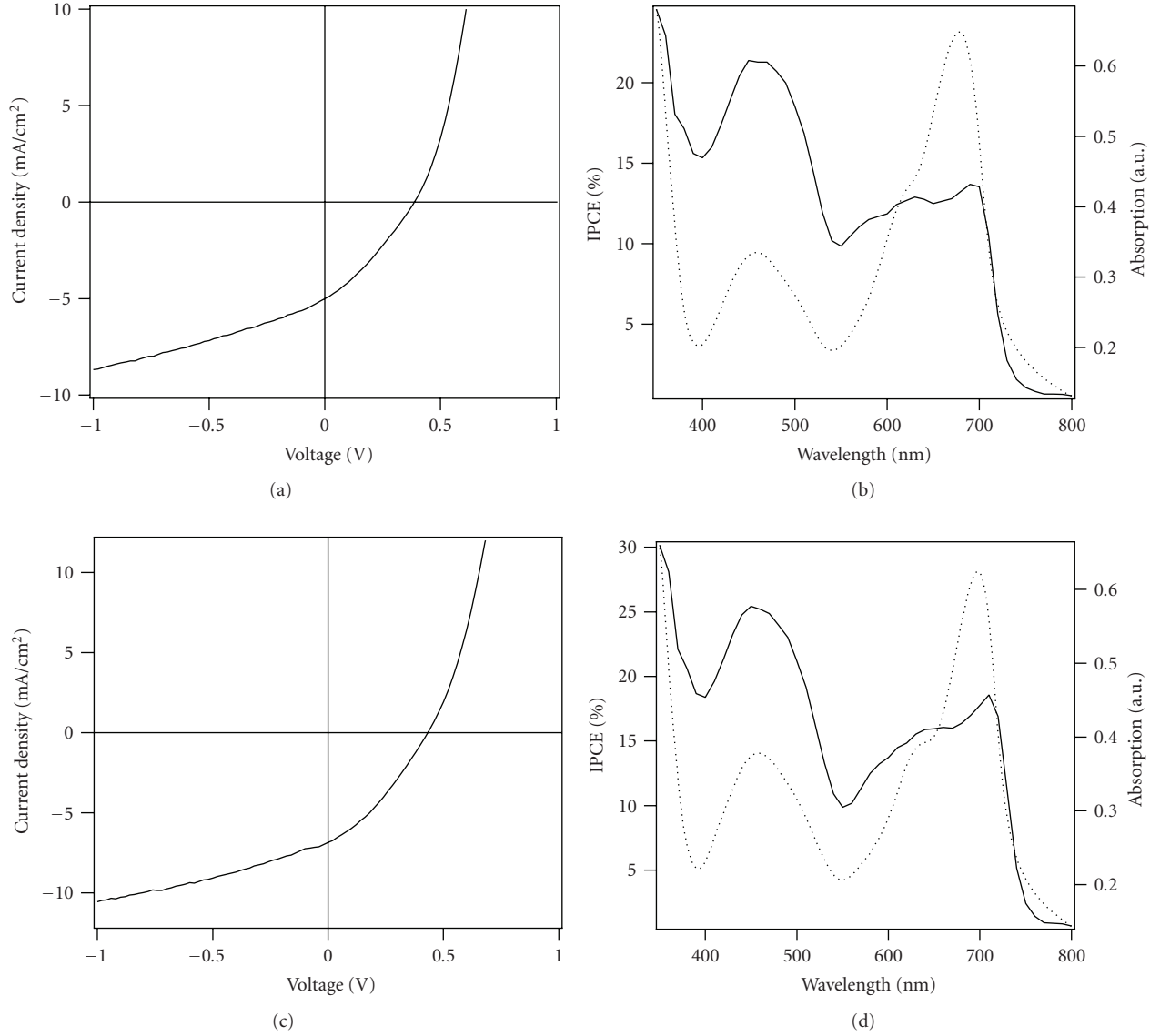


FIGURE 4: Current-voltage characteristics and IPCE curves for solar cells based on 20 nm thick SQ01 ((a) and (b)) and SQ02 ((c) and (d)) films. The dotted lines in (b) and (d) represent the absorption of SQ01 and SQ02 based cells, respectively.

of the dyes, the photovoltaic performance of SQ01 and SQ02 are rather similar. Both *J-V* curves show a typical S-shape behavior, which is somewhat dependent on the choice of the cathode. This feature could be induced by poor charge carrier transport in the squaraine layers. We do not exclude the possibility that a contact barrier at the anode interface could also lead to the S-shape feature. For both devices, the Ca cathode provides higher J_{SC} , FF, and slightly lower V_{OC} . We have attributed the better device performance to Ohmic contact formation between Ca and C₆₀. Al-C₆₀ contact generally introduces an energy barrier that hinders the electron extraction by the cathode. This barrier can be reduced significantly by introducing a thin buffer layer of Alq₃ [24]. In our devices, the charge extraction ability of the Ca cathode turns out to be still better than the Al cathode with Alq₃ buffer layer. The lowered V_{OC} could be explained

by the higher workfunction of the aluminum electrode as compared to the low workfunction of Ca [26–28].

The corresponding IPCE curves are shown in Figures 3(b) and 3(d) together with the absorption spectra of the cells. The IPCE of the cells using Ca cathodes are significantly higher than those using Al cathodes, indicating better charge extraction. The latter may also result from a higher built-in field produced in the devices using Ca cathodes. Strikingly, in the absorption region from 600 nm to 700 nm, the IPCE does not match the absorbance of the dye films. On the contrary, the minimum IPCE occurs at the maximum absorbance, which is also termed as antibatic behavior. Light irradiation penetrating through the ITO and PDOT:PSS layer is strongly absorbed when entering the dye layer, where excited states (excitons) are formed [29]. It appears that a large part of the excitons is not able to reach the charge separating

TABLE 1: Photovoltaic performance of SQ01- and SQ02-based solar cells using C_{60} as electron acceptor. Film thicknesses of 40 nm and 35 nm were used for SQ01 and SQ02, respectively. When ultrathin films were used, the thickness corresponds to 20 nm for both squaraine derivatives. The type of cathode utilized in the devices is also indicated.

	J_{SC} (mA/cm ²)	V_{OC} (V)	FF	η_p (%)
SQ01				
Al cathode	1.7	0.42	0.218	0.16
Ca cathode	2.6	0.38	0.229	0.23
Thin SQ film	5.0	0.38	0.312	0.59
SQ02				
Al cathode	2.0	0.46	0.228	0.21
Ca cathode	2.7	0.42	0.241	0.27
Thin SQ film	6.8	0.44	0.328	1.01

organic heterointerface, indicating that the exciton diffusion length is certainly smaller than the film thickness of SQ01 and SQ02. Even though fairly thin squaraine films were used, a substantial portion of the incoming light is merely filtered and cannot contribute to charge generation. As a consequence, the IPCE values in the absorption region of the squaraines are below 6%. The maximum IPCE locates between 450 nm and 500 nm, a spectral region where C_{60} is known to have a photocurrent peak [30]. As a matter of fact, the incident photons with wavelengths in the C_{60} absorption region are not filtered by the squaraine layer but are transmitted to the C_{60} layer where absorption occurs. In this process, the excited C_{60} molecule provides the possibility of electron transfer from the HOMO of the squaraine to the HOMO of C_{60} , resulting in the IPCE peak around 450 nm.

In order to improve device performance in squaraine-based bilayer devices, one possibility is to reduce the squaraine film thickness. Although less photons are being absorbed by the thinner film, a much larger proportion of excitons would be able to reach the organic heterointerface, resulting in a higher number of generated charges. In Figure 4, the performance of devices using 20nm thick squaraine dye films is shown. It has to be noted that decent diode characteristics were obtained despite the extremely small thickness of the dye films. Apparently, the squaraine derivatives used here own excellent film forming properties. In these devices, the IPCE in the absorption region of SQ01 and SQ02 reaches 12.8% and 18.5%, respectively. Moreover, the IPCE spectrum now resembles the absorption spectrum of the dye films. Again, this corroborates the fact that light filtering without charge generation is occurring for the thicker squaraine films. Additionally to improved charge generation, the reduced film thickness also leads to a better hole-transport through the squaraine film, and hence a smaller series resistance. Importantly, the S-shape, which is observed for the thicker squaraine layers, has been largely reduced when thin layers are employed. As demonstrated by J - V curves (Figures 4(a) and 4(c)), the J_{SC} and FF increase for both devices results in much better PCE of 0.59% for SQ01 and 1.01% for SQ02.

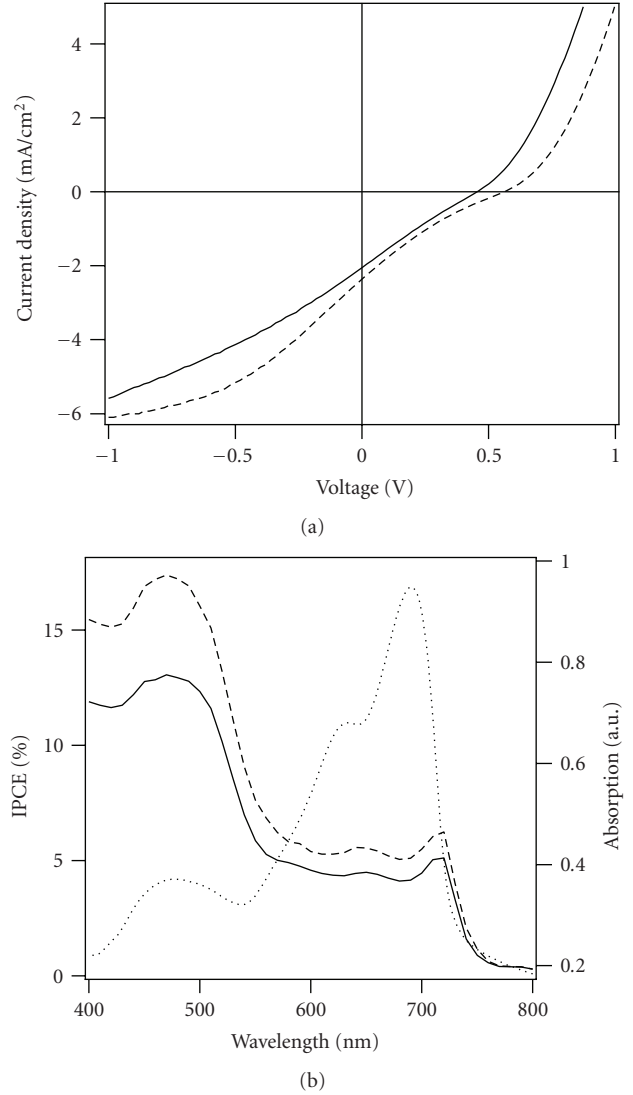


FIGURE 5: Current-voltage characteristics (a) and IPCE curves (b) of pristine (full line) and doped (dashed line) solar cells based on SQ02. The absorbance of the cell is also indicated (dotted line).

Charge transport in squaraine films has been investigated very scarcely in literature. In the crystalline state, a field effect hole mobility of $1 \times 10^{-3} \text{ cm}^2 \text{ V}^{-1} \text{ s}^{-1}$ was reported for a particular squaraine derivative [31]. As demonstrated by the authors, the mobility was strongly dependent on the morphology of the thin electroactive film. In the present work, we use assymetric squaraine dyes that moreover possess octyl chains. This particular chemical structure provides good solubility and is probably also responsible for good film forming properties. However, the particular structure of SQ01 and SQ02 may be unfavorable for charge transport and may be responsible for low charge carrier mobility.

In our previous work, we were able to increase the hole transport by doping the electron-donor film [25]. By introducing oxidative dopants, the film conductivity rises,

and hence more photogenerated charges can be extracted. We applied the same strategy in the case of SQ02-based devices. In order to evaluate the effect of doping, we focussed on the thicker SQ02 film of 35 nm, since the effect of conductivity is expected to be higher in this case. SQ02 was first doped in solution using NO^+BF_4^- as oxidizing agent before being coated on the PEDOT:PSS layer. We found that doping was not substantially enhancing device performance. The optimum doping concentration was obtained for an $\text{NO}^+\text{BF}_4^-/\text{SQ02}$ ratio of 0.005 (mol/mol). At higher concentration, doping has a deteriorating effect, probably due to defect formation in the organic layer. As shown in Figure 5, doping increases the current output (J_{SC} , IPCE) and open-circuit voltage (see Table 1). Similarly to our previous work, we believe that the increased V_{OC} is due to the formation of a Schottky barrier at the PEDOT:PSS/SQ02 interface upon equilibration of the respective Fermi levels.

4. Conclusion

In summary, we have fabricated a series of organic solar cells with squaraine dyes SQ01 and SQ02. The active organic layers form planar heterojunctions, where charge separation takes place between the squaraine electron donor and the C_{60} acceptor. Due to the extremely high extinction coefficients and the limited exciton diffusion length in squaraines, these devices show strong light filtering effects even at small film thicknesses of 35 nm to 40 nm. Only if the film thickness is reduced to 20 nm, power conversion efficiencies of 1% can be achieved. The photovoltaic performance is a result of both the photoactivity of C_{60} in the blue-to-green spectral domain and the photogeneration in the far red domain, where the squaraine dyes absorb. Further optimization of the devices would imply an increase of the hole carrier transport in the squaraine films. This conclusion is corroborated by the fact that oxidative doping of the dye film leads to increased J_{SC} and V_{OC} .

Acknowledgments

The Swiss Competence Center for Energy and Mobility CCEM-CH and "Swisselectric Research" are gratefully acknowledged for their financial support.

References

- [1] W. Ma, C. Yang, X. Gong, K. Lee, and A. J. Heeger, "Thermally stable, efficient polymer solar cells with nanoscale control of the interpenetrating network morphology," *Advanced Functional Materials*, vol. 15, no. 10, pp. 1617–1622, 2005.
- [2] J. Xue, B. P. Rand, S. Uchida, and S. R. Forrest, "A hybrid planar-mixed molecular heterojunction photovoltaic cell," *Advanced Materials*, vol. 17, no. 1, pp. 66–71, 2005.
- [3] P. Peumans, A. Yakimov, and S. R. Forrest, "Small molecular weight organic thin-film photodetectors and solar cells," *Journal of Applied Physics*, vol. 93, no. 7, pp. 3693–3723, 2003.
- [4] M. Riede, T. Müller, W. Tress, R. Schüppl, and K. Leo, "Small-molecule solar cells—status and perspectives," *Nanotechnology*, vol. 19, no. 42, Article ID 424001, 12 pages, 2008.
- [5] B. P. Rand, J. Genoe, P. Heremans, and J. Poortmans, "Solar cells utilizing small molecular weight organic semiconductors," *Progress in Photovoltaics: Research and Applications*, vol. 15, no. 8, pp. 659–676, 2007.
- [6] M. T. Lloyd, J. E. Anthony, and G. G. Malliaras, "Photovoltaics from soluble small molecules," *Materials Today*, vol. 10, no. 11, pp. 34–41, 2007.
- [7] F. Meng, K. Chen, H. Tian, L. Zuppiroli, and F. Nüesch, "Cyanine dye acting both as donor and acceptor in heterojunction photovoltaic devices," *Applied Physics Letters*, vol. 82, no. 21, pp. 3788–3790, 2003.
- [8] M. T. Lloyd, A. C. Mayer, A. S. Tayi, et al., "Photovoltaic cells from a soluble pentacene derivative," *Organic Electronics*, vol. 7, no. 5, pp. 243–248, 2006.
- [9] G. A. Chamberlain, "Organic solar cells: a review," *Solar Cells*, vol. 8, no. 1, pp. 47–83, 1983.
- [10] H. E. Sprenger and W. Ziegenbein, "Cyclobutenediylum dyes," *Angewandte Chemie International Edition*, vol. 7, pp. 530–535, 1968 (English).
- [11] K.-Y. Law, "Organic photoconductive materials: recent trends and developments," *Chemical Reviews*, vol. 93, no. 1, pp. 449–486, 1993.
- [12] K.-Y. Law and F. C. Bailey, "Squaraine chemistry. Synthesis, characterization, and optical properties of a class of novel unsymmetrical squaraines: [4-(dimethylamino)phenyl](4'-methoxyphenyl)squaraine and its derivatives," *Journal of Organic Chemistry*, vol. 57, no. 12, pp. 3278–3286, 1992.
- [13] C.-T. Chen, S. R. Marder, and L.-T. Cheng, "Syntheses and linear and nonlinear optical properties of unsymmetrical squaraines with extended conjugation," *The Journal of the American Chemical Society*, vol. 116, no. 7, pp. 3117–3118, 1994.
- [14] D. L. Morel, "Some aspects of the role of solid state chemistry in the performance of organic solar cells," *Molecular Crystals and Liquid Crystals*, vol. 50, no. 1–4, pp. 127–137, 1979.
- [15] A. Burke, L. Schmidt-Mende, S. Ito, and M. Grätzel, "A novel blue dye for near-IR 'dye-sensitized' solar cell applications," *Chemical Communications*, no. 3, pp. 234–236, 2007.
- [16] Md. K. Nazeeruddin, R. Humphry-Baker, M. Grätzel, et al., "Efficient near-IR sensitization of nanocrystalline TiO_2 films by zinc and aluminum phthalocyanines," *Journal of Porphyrins and Phthalocyanines*, vol. 3, no. 3, pp. 230–237, 1999.
- [17] S. Alex, U. Santhosh, and S. Das, "Dye sensitization of nanocrystalline TiO_2 : enhanced efficiency of unsymmetrical versus symmetrical squaraine dyes," *Journal of Photochemistry and Photobiology A*, vol. 172, no. 1, pp. 63–71, 2005.
- [18] C. Li, W. Wang, X. Wang, B. Zhang, and Y. Cao, "Molecular design of squaraine dyes for efficient far-red and near-IR sensitization of solar cells," *Chemistry Letters*, vol. 34, no. 4, pp. 554–555, 2005.
- [19] A. Otsuka, K. Funabiki, N. Sugiyama, T. Yoshida, H. Minoura, and M. Matsui, "Dye sensitization of ZnO by unsymmetrical squaraine dyes suppressing aggregation," *Chemistry Letters*, vol. 35, no. 6, pp. 666–667, 2006.
- [20] S. Hotchandani, S. Das, K. G. Thomas, M. V. George, and P. V. Kamat, "Interaction of semiconductor colloids with J-aggregates of a squaraine dye and its role in sensitizing nanocrystalline semiconductor films," *Research on Chemical Intermediates*, vol. 20, no. 9, pp. 927–938, 1994.
- [21] J.-H. Yum, P. Walter, S. Huber, et al., "Efficient far red sensitization of nanocrystalline TiO_2 films by an unsymmetrical squaraine dye," *Journal of the American Chemical Society*, vol. 129, no. 34, pp. 10320–10321, 2007.

- [22] F. Silvestri, M. D. Irwin, L. Beverina, A. Facchetti, G. A. Pagani, and T. J. Marks, "Efficient squaraine-based solution processable bulk-heterojunction solar cells," *Journal of the American Chemical Society*, vol. 130, no. 52, pp. 17640–17641, 2008.
- [23] T. Geiger, S. Kuster, J. H. Yum, et al., "Molecular design of unsymmetrical squaraine dyes for high efficiency conversion of low energy photon on TiO₂ nanocrystalline films," *Advanced Functional Materials*, vol. 19, pp. 734–738, 2007.
- [24] Q. L. Song, F. Y. Li, H. Yang, et al., "Small-molecule organic solar cells with improved stability," *Chemical Physics Letters*, vol. 416, no. 1–3, pp. 42–46, 2005.
- [25] B. Fan, R. Hany, J.-E. Moser, and F. Nüesch, "Enhanced cyanine solar cell performance upon oxygen doping," *Organic Electronics*, vol. 9, no. 1, pp. 85–94, 2008.
- [26] V. D. Mihailetschi, P. W. M. Blom, J. C. Hummelen, and M. T. Rispen, "Cathode dependence of the open-circuit voltage of polymer:fullerene bulk heterojunction solar cells," *Journal of Applied Physics*, vol. 94, no. 10, pp. 6849–6854, 2003.
- [27] D. Cheyns, J. Poortmans, P. Heremans, et al., "Analytical model for the open-circuit voltage and its associated resistance in organic planar heterojunction solar cells," *Physical Review B*, vol. 77, no. 16, Article ID 165332, 10 pages, 2008.
- [28] C. Uhrich, D. Wynands, S. Olthof, et al., "Origin of open circuit voltage in planar and bulk heterojunction organic thin-film photovoltaics depending on doped transport layers," *Journal of Applied Physics*, vol. 104, no. 4, Article ID 043107, 2008.
- [29] B. A. Gregg, S.-G. Chen, and R. A. Cormier, "Coulomb forces and doping in organic semiconductors," *Chemistry of Materials*, vol. 16, no. 23, pp. 4586–4599, 2004.
- [30] A. Geiser, B. Fan, H. Benmansour, et al., "Poly(3-hexylthiophene)/C₆₀ heterojunction solar cells: implication of morphology on performance and ambipolar charge collection," *Solar Energy Materials and Solar Cells*, vol. 92, no. 4, pp. 464–473, 2008.
- [31] E. C. P. Smits, S. Setayesh, T. D. Anthopoulos, et al., "Near-infrared light-emitting ambipolar organic field-effect transistors," *Advanced Materials*, vol. 19, no. 5, pp. 734–738, 2007.